ChemPubSoc Europe

DOI: 10.1002/chem.201701576

CHEMISTRY A European Journal Full Paper

Organocatalysis

Complexity in Acid–Base Titrations: Multimer Formation Between Phosphoric Acids and Imines

Christian Malm, Heejae Kim, Manfred Wagner, and Johannes Hunger*[a]

Abstract: Solutions of Brønsted acids with bases in aprotic solvents are not only common model systems to study the fundamentals of proton transfer pathways but are also highly relevant to Brønsted acid catalysis. Despite their importance the light nature of the proton makes characterization of acid–base aggregates challenging. Here, we track such acid–base interactions over a broad range of relative compositions between diphenyl phosphoric acid and the base quinaldine in dichloromethane, by using a combination of dielectric relaxation and NMR spectroscopy. In contrast to what one would expect for an acid–base titration, we find strong deviations from quantitative proton transfer from the acid to the base. Even for an excess of the base, multimers consisting of one base and at least two acid molecules are formed, in addition to the occurrence of proton transfer from the acid to the base and simultaneous formation of ion pairs. For equimolar mixtures such multimers constitute about one third of all intermolecular aggregates. Quantitative analysis of our results shows that the acid-base association constant is only around six times larger than that for the acid binding to an acid-base dimer, that is, to an already protonated base. Our findings have implications for the interpretation of previous studies of reactive intermediates in organocatalysis and provide a rationale for previously observed nonlinear effects in phosphoric acid catalysis.

Introduction

Solutions of Brønsted acids with bases have been intensively studied as model systems to understand the fundamentals of for example, strong hydrogen-bonding,[1–5] proton transfer pathways,[6–8] Brønsted acid organocatalysis,[9–13] or mechanisms of enzymatic activity.[14] In general, upon association of an acid and a base, the proton is shared between the two molecules and the quantum nature of the light proton results in substantial delocalization of the proton between the acidic and the basic group.[15] This delocalization also limits the experimental and computational methods that are suitable to study such interactions. Experimentally, valuable insight into the location of the proton and as such the nature of the bond between the acids and bases has been obtained from nuclear magnetic resonance (NMR) experiments at reduced temperatures.[6,10,14] For specific acids and bases the information obtained using NMR has been complemented by optical or vibrational spectroscopies.[4,6,7] To date many studies have focused on carboxylic acids and it has been concluded that the nature of this strong bond varies between a hydrogen-bonded complex with the proton located in the proximity of the acid and an ion pair (full proton transfer), depending on the chemical nature of the acid and the base.[6]

The interaction of phosphoric acid derivatives with organic imine bases in aprotic solvents has only in recent years received increasing attention, as these acid-base combinations are highly relevant to the emerging field of (asymmetric) organocatalysis.[16–19] Analogously to carboxylic acids, the interaction of such phosphoric acids with various imines has been studied using both computational[20–23] and experimental[9–12,20,22] methods. It has remained challenging, however, to study complexes formed between phosphoric acids and imines at conditions that are relevant to the catalytic process: For instance, with computational approaches the solvent is typically approximated by a continuum[21] and NMR experiments are mostly performed at temperatures below the reaction temperature.[9,10,13] We have recently shown using a combination of dielectric relaxation spectroscopy (DRS), NMR spectroscopy, and ab initio calculations that the nature of catalyst–substrate interaction can be elucidated at catalytically relevant temperatures and in a range of molecular solvents.[11] By studying equimolar solutions of a substituted phosphoric acid and quinaldine, an aromatic heterocycle, we could show that the interaction is dominated by proton transfer from the acid to the base and subsequent formation of ion pairs. The dissociation of these ion pairs into free ions is correlated with a reduced enantioselectivity in the catalytic process. In contrast to some earlier

[a] C. Malm, Dr. H. Kim, Dr. M. Wagner, Dr. J. Hunger
Department of Molecular Spectroscopy
Max Planck Institute for Polymer Research
Ackermannweg 10, 55128 Mainz (Germany)
E-mail: hunger@mpip-mainz.mpg.de

Supporting information and the ORCID identification number(s) for the author(s) of this article can be found under https://doi.org/10.1002/chem.201701576.

reports,[10] the dominant formation of ion pairs as intermediates has been recently confirmed using NMR experiments.[13]

While these recent studies[9–11,13] have advanced our understanding of the interaction between phosphoric acids and imine bases, these studies were limited to equimolar solutions of acids and bases. Under realistic catalytic conditions, however, only a few mole percent of acid is added as catalyst.[18] Also computational approaches typically consider only one substrate and one catalyst molecule,[24] which limits such studies to a single bimolecular reaction pathway. Experimentally however, there is evidence for the formation of more than one intermediate between the acid and the base.[10] In order to understand the catalytic mechanism it is vital to explore which intermediates are formed at compositions comparable to the catalytic process. Correlating the properties of the formed intermediates to the catalytic activity has the potential to improve prediction of catalyst performance,[12,25] as current approaches rely on the average properties of all acids and/or bases in solution (e.g. the averaged NMR chemical shift[12,25] or vibrational frequencies[25]).

In order to investigate the intermediate that is the dominant species at compositions relevant to catalysis, we herein report a detailed study on the interaction between a substituted phosphoric acid (diphenyl phosphoric acid, DPP) and an aromatic imine (quinaldine, Qu) dissolved in dichloromethane at ambient temperature, which is relevant to the transfer hydrogenation reaction catalyzed by phosphoric acids (see Figure 1).[26] By using a combination of dielectric relaxation and

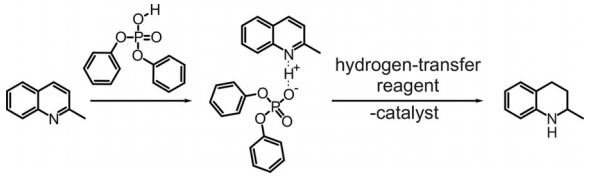

Figure 1. Reaction scheme of the Brønsted acid catalyzed transfer hydrogenation. The catalyst (diphenyl phosphoric acid) activates the imine (quinaldine), followed by hydrogenation yielding tetrahydroquinaldine.

NMR spectroscopy, we particularly focus on the effect of the ratio between the DPP and Qu dissolved in dichloromethane. We find that at low concentrations of acid, Qu and DPP predominantly aggregate to bimolecular QuH^+–DPP^- ion pairs. With increasing concentration of DPP, multimers (e.g. QuH^+–DPP^-–DPP) are formed to a significant extent and for the commonly studied equimolar samples these multimers constitute more than 30% of the observed molecular aggregates between DPP and Qu.

Results and Discussion

NMR titration experiments

To study the interaction between Qu and DPP as a function of their molar ratio in dichloromethane, we performed a titration experiment: In all samples the concentration of Qu was kept constant at $c_{Qu} = 0.1\ mol\,L^{-1}$, while the concentration of DPP was varied such that we cover both, samples with an excess of Qu and an excess of DPP. As we have shown previously, the ^1H NMR chemical shift of protons of Qu is very sensitive to protonation of Qu by DPP.[11] Hence, to monitor the proton transfer in the titration experiment, we recorded the ^1H NMR spectra of Qu with simultaneously increasing c_{DPP} from 0.01 $mol\,L^{-1}$ to 0.5 $mol\,L^{-1}$. As can be seen from the chemical shift of the H4 proton of Qu, δ_{H4}, (located opposite to the nitrogen atom in the six-membered heterocycle, see inset of Figure 2a), the

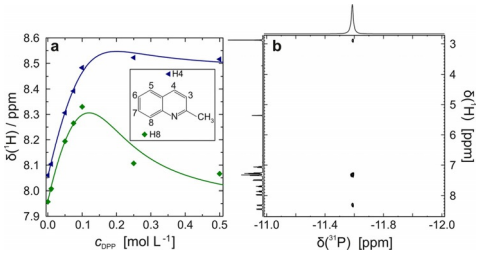

Figure 2. a) Chemical shift of the protons H4 and H8 of Qu as a function of DPP concentration at a constant Qu concentration of 0.1 $mol\,L^{-1}$: the proton in close proximity to the nitrogen (H8) shows an increased shielding with increasing excess of acid, while the chemical shift of H4 nearly exhibits the sigmoidal behavior that would be expected for acid–base titrations. Symbols correspond to experimental data and solid lines show the description with the association model (Equation (6) see text). b) HOESY spectrum of an equimolar (0.1 $mol\,L^{-1}$) solution of DPP and Qu. Cross-peaks evidence proximity of the phosphor not only to the phenyl groups (7.3 ppm) of the DPP but also to H8 (8.3 ppm) and the methyl group H9 (2.9 ppm) of Qu. Note, that small signals in the ^1H spectra at 6.9, 6.7, and 3.7 ppm originate from a minor impurity, presumably *p*-anisidine, which does not affect our conclusions.

variation of the chemical shift is in accordance to what one would expect for titration of a base with an acid (Figure 2a): At $c_{DPP} \leq c_{Qu}$ the value of δ_{H4} increases with increasing concentration of acid, in line with a partial protonation of some Qu molecules and δ_{H4} representing the (motionally) averaged chemical shift of Qu and QuH^+. The increase of δ_{H4} therefore reflects a reduction of the shielding of this specific proton, which can be readily related to a reduction of the average electron density in the vicinity of the H4 proton upon protonation of Qu. For samples with an excess of DPP $c_{DPP} > 0.1\ mol\,L^{-1}$ the δ_{H4} values reach a plateau, which suggests that an excess of DPP does hardly affect the electronic environment of H4 (i.e. quantitative protonation of all Qu). In analogy to the observations for H4, also the chemical shifts for protons H3–H7 exhibit similar trends (see Supporting Information, Figure S1). The magnitude of the variation amongst H3–H7 is however largest for H4 (Figure S1), which is in line with this position being the initial reactive center for the hydride transfer in the hydrogenation reaction (Figure 1).[37]

Conversely, the chemical shift of H8 varies markedly different with increasing concentration of DPP: At $c_{DPP} \leq c_{Qu}$ the value of δ_{H8} increases—similar to our findings for H3–H7. However, at $c_{DPP} > 0.1\ mol\,L^{-1}$ the value for δ_{H8} shows a pronounced decrease with increasing concentration of DPP. At $c_{DPP} =$

0.5 mol L^{-1} the value of δ_{H8} nearly assumes the values close to neat solution of Qu (in the absence of any acid). We note that we find a similar behavior for the chemical shift of the methyl group δ_{H9} (see Figure S2, Supporting Information). Our results thus show that an excess of DPP increasingly shields the protons H8 and the methyl group H9, relative to the equimolar mixture of DPP and Qu.

Hence, the NMR titration experiment demonstrates that only at $c_{DPP} \ll c_{Qu}$, the observed chemical shift is dominated by deprotonation of DPP and the corresponding partial protonation of Qu. With increasing concentration of DPP the shielding of protons of Qu in the direct vicinity of the aromatic nitrogen (H8 and methyl group H9) however deviates from what one would expect for quantitative, bimolecular proton transfer between Qu and DPP.

To explore the origin of the counterintuitive shielding of H8 and H9 we use HOESY. This technique is sensitive to through space interactions (~ < 5 Å) between phosphor nuclei and protons (also in absence of coupling through a chemical bond). Such a two-dimensional ^{31}P–^{1}H HOESY spectrum (Figure 2b) shows three pronounced cross-peaks: The most intense cross-peak is due to the intramolecular interaction between the ^{31}P ($\delta_{^{31}P} = -11.6$ ppm) and the phenyl groups of the DPP ($\delta_{^{1}H,\,phenyl} \approx 7.3$ ppm). More importantly, we find two additional intermolecular cross-peaks evidencing interaction with Qu: The HOESY spectrum for an equimolar solution of DPP and Qu show interaction of the ^{31}P nuclei with protons located at $\delta_{H8} = 8.3$ ppm and $\delta_{H9} = 2.9$ ppm for Qu, the two signals that show the decrease in chemical shift upon adding an excess of DPP. Thus, the HOESY spectrum provides strong evidence that the peculiar behavior of H8 and H9 for an excess of DPP in the titration experiment can be traced back to DPP in the direct proximity of these protons, that is, the formation of molecular aggregates between QuH^+ and DPP^-. This observation is in line with our previous study,[11] where we could show that the dielectric spectra of equimolar solutions are dominated by QuH^+–DPP^- ion pairs.

Dielectric relaxation spectroscopy

Accordingly, to obtain further insight into the species that are formed in solution as a function of the molar ratio between Qu and DPP, we perform DRS experiments with varying sample composition. In general, DRS spectra are dominated by the rotation of molecular level dipoles. As ion pairs (e.g. QuH^+–DPP^- ion pairs[11]) have an intrinsically large electrical dipole moment, DRS is particularly sensitive to the formation of ion pairs.[38] In Figure 3a we show the complex permittivity spectra for solutions containing 0.1 mol L^{-1} Qu with varying concentration of DPP. All spectra show a relaxation process, which is characterized by a dispersion in the dielectric permittivity, $\varepsilon'(\nu)$, and a peak in the dielectric loss, $\varepsilon''(\nu)$, centered at ≈70 GHz.

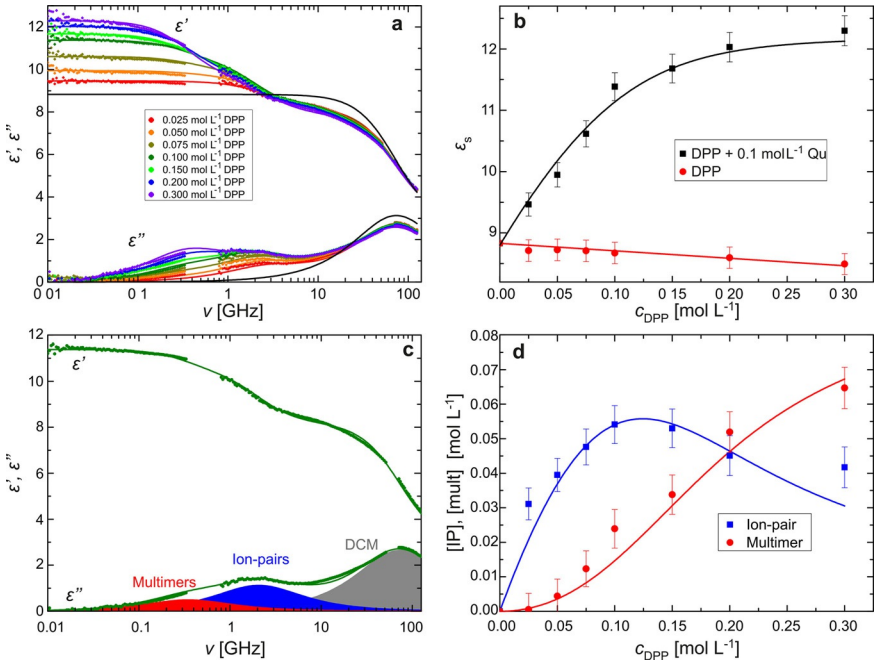

Figure 3. a) Dielectric permittivity, $\varepsilon'(\nu)$, and dielectric loss spectra, $\varepsilon''(\nu)$, for solutions of 0.1 mol L^{-1} Qu with varying concentration of DPP. Symbols show experimental data and lines show the fit of Eq. 1 to the spectra. The black solid line shows the dielectric spectrum of the solvent, dichloromethane, which was taken from literature.[39] Note that for visual clarity the contribution due to the Ohmic loss (last term of Equation (1)) has been subtracted. b) Extrapolated static permittivity, ε_s, vs. concentration of DPP for solution of neat DPP (red symbols) and solutions containing 0.1 mol L^{-1} Qu (black symbols). Error bars are estimated to 0.02 ε_s.[38] Solid lines are a visual aid. c) Dielectric spectrum of an equimolar mixture of DPP and Qu. Symbols show experimental data and the solid lines show the fits using Eq. 1. Shaded areas indicate the contribution of the three relaxation modes (multimer, ion pair, and solvent) to the dielectric loss (see Equation (1)) d) Calculated concentrations of ion pairs (blue squares) and multimers (red circles) as extracted from the dielectric relaxation amplitudes (for details see text and Supporting Information). Error bars were estimated assuming an uncertainty of 0.02 ε_s[38] in the relaxation strength. Solid lines show fits of the association model (Equations (4) and (5)) to the data. Note that the deviations of the fit from that data at $c_{DPP} = 0.3$ mol L^{-1} can be related to the neglect of aggregates larger than trimers in Equations (4) and (5).

This relaxation mode can be readily assigned to the rotational diffusion of the dipolar solvent dichloromethane (see also black solid lines in Figure 3a).[39] Besides a minor reduction in relaxation amplitude of this mode due to the decreasing volume concentration of dichloromethane with increasing solute concentration, the relaxation of dichloromethane is nearly unaffected by the addition of DPP, which indicates that the added solute does not bind dichloromethane strongly in its solvation shell. The addition of DPP to the quinaldine solution leads to the appearance of at least one broad relaxation in the range centered at about 2 GHz. Thus, this relaxation can be assigned to be due to the solutes and its amplitude is increasing with increasing DPP concentration. The increasing amplitude goes along with an increase in the limiting permittivity at low frequencies ($\varepsilon_s = \lim_{\nu\to 0} \varepsilon'(\nu)$), that is, the static dielectric constant. As can be seen in Figure 3b, the static permittivity of the samples monotonically increases with increasing concentration of DPP (black symbols in Figure 3b). This observation is in stark contrast to solutions of only DPP in dichloromethane (in the absence of Qu), where the static permittivity decreases with increasing concentration of acid (red symbols in Figure 3b, see also Supporting Information Figure S3). In general, the static dielectric constant is a measure of the volume concentration of electrical dipoles (multiplied by their squared electrical dipole moment, see also below).[40] Thus, the increase of ε_s with increasing c_{DPP} for solutions containing Qu indicates the formation of dipolar aggregates upon addition of DPP over the entire concentration range of the present study. Contrarily, our data suggest that addition of DPP does not go along with the formation of dipolar species in the absence of quinaldine. Notably, ε_s exhibits a steep increase at low concentrations of DPP ($c_{DPP} < 0.1$ mol L^{-1}), while the slope of ε_s vs. c_{DPP} is reduced for an excess of DPP ($c_{DPP} > 0.1$ mol L^{-1}). Hence, in line with the interaction of DPP and Qu at all studied concentrations as concluded from Figure 2, the values of ε_s indicate that dipolar species are formed and/or the electrical dipole moment of these species is increased upon adding DPP over the entire concentration range of the present study.

In order to quantitatively analyze the dielectric spectra, we fit a relaxation model to the spectra consisting of multiple relaxation modes to the spectra. This model obviously contains contributions due to the solvent at 70 GHz (2 ps).[39] The relaxation of the solute between 0.1 and 5 GHz has an asymmetric shape and its symmetry varies with concentration of DPP: while the maximum in ε'' is located at around 2 GHz for low concentrations of DPP, a pronounced shoulder appears at around 0.4 GHz at high concentrations of DPP. This asymmetry provides evidence for the presence of at least two relaxation modes due to the solutes. Due to the prevalence of the 2 GHz relaxation mode at low c_{DPP} (see also below), we assign this relaxation mode to the smallest conceivable aggregate between Qu and DPP: QuH^+–DPP^- ion pairs (see also [11]).[41] As the peak position in dielectric spectra is determined by the molecular volume of the rotating dipoles (and the sample's viscosity),[39,40] the location of the second solute relaxation mode at 0.4 GHz suggests that these dipolar species have a larger molecular volume (compared to the ion pairs). We therefore assign this lower frequency relaxation to the rotation of multimers (at least QuH^+–DPP^-–DPP trimers) formed between DPP and Qu.

Hence, we use a combination of three (Debye-type) relaxation modes[42] to describe the experimental spectra, which is the model with the least number of parameters that gave a consistent description of the experimental data:

$$\hat{\varepsilon}(\nu) = \frac{S_{mult}}{1 + 2\pi i\nu\tau_{mult}} + \frac{S_{IP}}{1 + 2\pi i\nu\tau_{IP}} + \frac{S_{DCM}}{1 + 2\pi i\nu\tau_{DCM}} + \varepsilon_\infty + \frac{\kappa}{2\pi i\nu\varepsilon_0} \quad (1)$$

where S_j and τ_j are the relaxation amplitudes (relaxation strengths) and relaxation times, respectively, with $j =$ mult (multimer), IP (ion pair), or DCM (dichloromethane). ε_∞ is the limiting permittivity at infinite frequencies, which accounts for all polarization components that are resonant at frequencies above the frequency range of the present study (e.g. due to electronic polarization or vibrational resonances). The last term of Equation (1) accounts for Ohmic losses resulting from the electrical conductivity, κ, and ε_0 is the permittivity of free space. Here, we assume κ, which is rather small for the present samples ($\kappa < 0.02$ S m^{-1} see Supporting Information Table S3), to be real and independent of frequency (i.e. the dc conductivity of the sample).

As can be seen from Figure 3a, Equation (1) excellently describes the experimental spectra over the entire frequency range at all studied concentrations. The contribution of the three relaxation modes to the dielectric loss spectrum are shown as shaded areas in Figure 3c and the obtained fit parameters are summarized in the Supporting Information (Table S3 and Figure S4). From these fits we find the relaxation time of DCM, $\tau_{DCM} \approx 2.1$ ps is largely unaffected by the presence of solute molecules. The relaxation amplitude S_{DCM} is slightly decreasing with increasing c_{DPP}, which can be related to the reduction (dilution) of the molar concentration of DCM upon adding DPP. Similar to τ_{DCM}, the ion pair relaxation time τ_{IP} does not vary substantially with varying c_{DPP}. Despite the multimer relaxation is detectable at all studied concentrations, the parameters associated with the multimers (τ_{mult}, S_{mult}) are due to the weak contribution of multimers at $c_{DPP} < 0.1$ mol L^{-1} somewhat scattered (see Figure S4). To reduce the scatter in the data at $c_{DPP} \leq 0.1$ mol L^{-1}, we fix τ_{mult} to 458 ps, which is the average value obtained at $c_{DPP} > 0.1$ mol L^{-1}, where S_{mult} is the dominant solute relaxation. This constraint has however little effect on the obtained values of S_{mult} (see Figure S4).

The relaxation amplitudes S_{IP} and S_{mult} can be directly related to the concentration of dipolar species, $[j]$ and their squared dipole moment ($S_j \sim [j]\mu_j^2$, $j =$ mult, IP).[11] To extract the molar concentrations of ion pairs, [IP], and multimers, [mult], we obtain the electrical dipole moments (μ_j) by assuming that at $c_{DPP} > 0.1$ mol L^{-1} all Qu molecules form either ion pairs or multimers and at $c_{DPP} < 0.1$ mol L^{-1} all DPP molecules from either QuH^+–DPP^- ion pairs or QuH^+–DPP^-–nDPP multimers (see Supporting Information). With these boundary conditions we find the electrical dipole moments of the ion pair and of multimers to be very similar: $\mu_{mult} = 21.4$ D and $\mu_{IP} = 21.5$ D (for de-

tails see Supporting Information, Figure S5). The notion that the dipole moment of a QuH^+–DPP^- ion pair is virtually unaffected upon association of an additional DPP molecule to the ion pair (formation of a QuH^+–DPP^-–DPP trimer) is also supported by ab initio calculations (see Supporting Information, Figure S6). As can be seen from Figure 3d, the thus obtained values for [IP] increase at low c_{DPP} and reach a maximum at $c_{DPP} \approx 0.1$ mol L^{-1} after which they decrease. The concentration of multimers, [mult], shows a sigmoidal shape with an inflection point at $c_{DPP} \approx 0.15$ mol L^{-1}. Notably, these results indicate that multimers are present at all concentrations and for an equimolar concentration about around 30% of all aggregates in solution are multimers. Hence, despite at low DPP concentrations a substantial amount of the base Qu is available, added acid (DPP) does not quantitatively protonate the base, but some fraction of DPP is bound in multimers.

Association model

To quantitatively describe the concentration dependence of ion pairs and multimers as shown in Figure 3d, we use an association model. For convenience we take only the formation of ion pairs (IP, QuH^+–DPP^-) and association of one additional DPP molecule to an ion pair resulting in a trimer (QuH^+–DPP^-–DPP) into account [Eq. (2), Eq. (3)]:

$$Qu + DPP \rightleftharpoons \{QuH^+DPP^-\} \quad (2)$$

$$\{QuH^+DPP^-\} + DPP \rightleftharpoons \{QuH^+DPP^-DPP\} \quad (3)$$

Here we neglect dissociation of ion pairs into free ions, as the number of free ions is very small in dichloromethane.[11] Accordingly, the relevant apparent association equilibria, which are based on concentrations rather than thermodynamic activity, are defined as [Eq. (4), Eq. (5)]:

$$K_1 = \frac{[IP]}{[Qu][DPP]} \quad (4)$$

$$K_2 = \frac{[mult]}{[IP][DPP]} \quad (5)$$

where [Qu] and [DPP] are the concentrations of free quinaldine and free DPP, respectively. K_1 and K_2 are the corresponding apparent association constants. Together with mass conservation ($c_{DPP} = [DPP] + [IP] + 2[mult]$, and $c_{Qu} = [Qu] + [IP] + [mult]$), this model can describe the observed concentration dependence of [IP], and [mult] very well (see solid lines in Figure 3d) with association constants $K_1 = 104$ L mol^{-1} and $K_2 = 16$ L mol^{-1}. Remarkably, these apparent equilibrium constants, which were obtained from our DRS results, can also describe the NMR chemical shifts as shown in Figure 2: assuming that the observed chemical shift δ is the concentration weighted average of all three species in solution:

$$\delta = \delta_{Qu}\frac{[Qu]}{c_{Qu}} + \delta_{IP}\frac{[IP]}{c_{Qu}} + \delta_{mult}\frac{[mult]}{c_{Qu}} \quad (6)$$

where δ_{Qu}, δ_{IP}, and δ_{mult} are the chemical shifts of free Qu, the ion pair, and the multimer, respectively. As can be seen from the solid lines in Figure 2a, also the chemical shifts of δ_{H4} and δ_{H8} (for other protons see Supporting Information) can be described by this association models with $K_1 = 104$ L mol^{-1} and $K_2 = 16$ L mol^{-1}, hence confirming that the two equilibria can describe the interaction of DPP and Qu at all studied concentrations. Only for a large excess of DPP ($c_{DPP} \geq 0.3$ mol L^{-1}) the model somewhat deviates from the experimental data (see Figure 2a and Figure 3d), which can be explained from the model being limited to formation of ion pairs and trimers (i.e. it does not account for other multimers). The chemical shifts for neat Qu, ion pairs and trimers, calculated by fitting the NMR titration data using Equation (6) can be found in Table S1 (see Supporting Information).

Diffusion ordered NMR experiments

To confirm this association behavior we perform diffusion ordered NMR spectroscopy (DOSY) for solutions containing 0.1 mol L^{-1} Qu at different concentrations of DPP. With DOSY we can relate the (motionally averaged) signals in the ^{1}H NMR spectra to the diffusivity of these protons (averaged over all species that are present in solution). As the diffusivity of the proton (i.e. the molecule or intermolecular aggregate) scales with the hydrodynamic volume, DOSY provides information on the average size of the aggregates in solution. In general, the signals at 7–7.5 ppm can be related to DPP, while protons with chemical shifts ranging from 7.5–9 ppm stem from Qu (Figure 4a). For mixtures with $c_{DPP} = 0.1$ mol L^{-1} and $c_{DPP} = 0.05$ mol L^{-1} the average diffusivity of DPP-containing species is lower than the average diffusivity of Qu containing species. This difference is consistent with the association model (Equation (6)), where we find that at these concentrations all DPP molecules are incorporated in intermolecular aggregates (ion pairs or multimers) with large molecular volumes (slow diffusion rates). Simultaneously a significant fraction of free Qu molecules is present for these compositions. As these free Qu molecules have a low hydrodynamic volume, compared to ion pairs or multimers, the presence of free Qu molecules reduces the average diffusivity of all Qu species at these concentrations. Only for an excess of DPP ($c_{DPP} = 0.5$ mol L^{-1}) all Qu molecules form aggregates with DPP and thus similar diffusivities of protons related to Qu and DPP are observed (Figure 4b).

Conclusion

Using a combination of dielectric relaxation and NMR experiments, we show that in solutions of Qu and DPP different intermolecular aggregates are formed, depending on the ratio between the base Qu and the acid DPP. In our titration experiment, multimers containing one QuH^+ cation, one DPP^- anion, and at least one more DPP molecule are formed. We find such multimers—similar to what has been suggested for carboxylic acids[3]—even for solutions containing an excess of Qu. Our results indicate that the electrical dipole moment of these multimers is very similar to that of QuH^+–DPP^- ion pairs, thus pro-

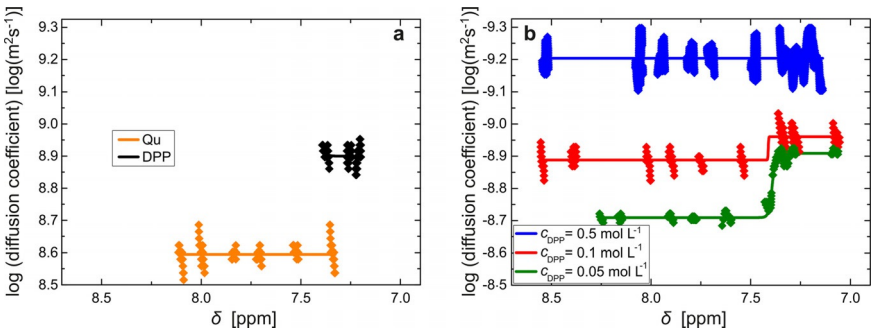

Figure 4. a) DOSY experiments for solutions of only Qu and only DPP. b) DOSY experiments for mixtures containing 0.1 mol L^{-1} Qu with varying concentrations of DPP at 298 K: Signals at >7.5 ppm correspond to Qu, while signals <7.5 ppm originate from the phenyl groups of DPP. The diffusion coefficient of Qu is decreased in the presence of small amounts of DPP. With increasing DPP concentration the diffusion coefficients of Qu and DPP become equal. Symbols show experimental data and solid lines are a visual aid.

viding evidence for the average location of the negative charge being not affected by the additional DPP molecule. As the NMR experiments show that the additional DPP molecule in the multimers is close to the positively charged NH^+ group of QuH^+, we propose that in the simplest multimer—the trimer—the negative charge is delocalized between the two hydrogen-bonded DPP molecules (Figure 5). Such intermolecular interaction between two DPP molecules in fact closely resembles the dimers of Brønsted acid that have been reported to prevail in weakly polar solvents.[3,43] Two association equilibria accounting for formation of Qu^+–DPP^- ion pairs and Qu^+–DPP^-–DPP trimers can describe the interaction of DPP and Qu at all studied concentrations. Remarkably, the association constant for DPP associating with a free quinaldine molecule ($K_1 = 104\ L\,mol^{-1}$) to form a Qu^+–DPP^- ion pair is only around 6 times higher than the association of DPP to a Qu^+–DPP^- ion pair ($K_2 = 16\ L\,mol^{-1}$) to form a multimer. This interplay between the two competing association paths is likely very sensitive to the solvent, and thus may explain the very different formation of intermolecular aggregates for other polar, aprotic solvents.[11] We observe these species (ion pairs and multimers) as separate relaxations in DRS, while their formation leads to motionally averaged signals in NMR. Thus, our results indicate that the lifetime of these aggregates (i.e. the time they exist before the intermolecular bond is broken) is shorter than a few milliseconds (NMR timescale) but longer than a few hundreds of picoseconds (the rotation time in DRS). As the formation of multimers is detected at all concentrations, our results imply that the ratio between the catalyst and the substrate is crucial in order to study reactive intermediates in organocatalysis. The simultaneous presence of different intermediates reported for equimolar mixtures[10] is very likely related to the presence of ion pairs and multimers in equimolar solutions. Moreover, our results show that in the catalytic process where typically a few mole percent of the phosphoric acid are added to the imine base,[26] ion pairs are the prevailing intermediates and thus ion pairs are very likely the active species in catalysis.[18] Our results also show that multimers are formed at all concentrations even for an excess of base. Based on our association model, these multimers constitute about 1.5 and 0.7% of all aggregates at molar ratios of 1:10 and 1:20 (DPP:Qu), which are typical catalyst loadings in organocatalysis. Since a minor species can be decisive for catalysis (Curtin–Hammet principle),[23] these multimers may nevertheless have catalytic significance. In fact, the few mole percent of phosphoric acid that is typically added to the substrate in the organocatalytic process is significantly more than what is used in transition metal catalysis.[44,45] Indeed, there is evidence for strong non-linear effects in phosphoric acid catalysis when around 10% of catalyst is added, which could only be explained by the activation of the substrate by more than one acid molecule.[46] Similarly, the association of two phosphoric acid molecules at a Ca^{2+} ion has been suggested to be of catalytic relevance[47] and in recent years catalysts that bear two phosphoric acid moieties on the same molecule[48–50] have been shown to provide superior catalytic activity. In this work we provide a route to identify the different intermediates that are formed in solution and to extract their respective properties: we obtained separately the electronic structure of the ion pairs and of the multimers from their extracted NMR chemical shifts and the DRS detected electrical dipole moment. Direct correlation of such electronic properties of these intermediates to the catalytic activity can provide mechanistic insight and thus improve prediction of catalytic activity based on their isolated electronic properties.[12,25]

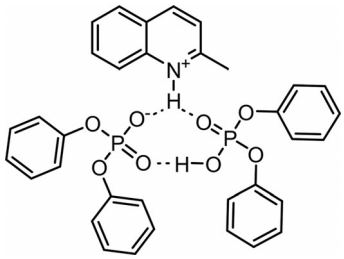

Figure 5. Proposed structure of the trimer, consisting of a quinaldinium cation, a diphenyl phosphate anion, and a diphenyl phosphoric acid.

Experimental Section

Diphenyl phosphoric acid (DPP) was purchased from Sigma–Aldrich and dried in vacuo ($<2\times10^{-2}$ mbar) for at least 8 hours. Quinaldine (Qu) was obtained from Sigma–Aldrich and used without further purification. The solvents dichloromethane (CH_2Cl_2, ACS reagent grade, Sigma–Aldrich) and deuterated dichloromethane (CD_2Cl_2, Carl Roth) were stored over molecular sieve (4 Å) and filtered using a 0.2 μm Omnipore membrane filter prior to use. Stock solutions of DPP and Qu were prepared by weighing the appropriate amount DPP or Qu into a volumetric flask and dissolving the solute in dichloromethane. Samples with different stoichiometric ratios between Qu and DPP were prepared, by mixing the corresponding volume of both stock solutions and the solvent using graduated glass pipettes. For NMR experiments a total sample volume of 1 mL was prepared for each sample using CD_2Cl_2. For DRS experiments we prepared samples with a total volume of 4 mL using CH_2Cl_2.

To study the formation of dipolar aggregates in solution, we use DRS,[27,28] which measures the polarization of these samples in an externally applied oscillating electric field with field frequency, ν. The induced polarization is experimentally measured and can be expressed in terms of the complex permittivity $\hat{\varepsilon}(\nu)$: [Eq. (7)]

$$\hat{\varepsilon}(\nu) = \varepsilon'(\nu) - i\varepsilon''(\nu) \tag{7}$$

with the real part, ε', being the frequency dependent permittivity and the imaginary part, ε'', representing the dielectric loss (i.e. absorption).[27,29] DRS spectra were recorded at frequencies ranging from 10 MHz to 110 GHz, using an Anritsu MS4647A Vector Network Analyzer. To cover this broad frequency range data obtained using several experimental geometries were combined. Frequencies at 54 to 110 GHz were covered using a coaxial reflectometer based on an external frequency converter module (Anritsu 3744A mmW module) and an open-ended coaxial probe based on 1 mm coaxial connectors.[30,31] Spectra at 0.8–50 GHz were recorded using an open-ended coaxial cell based on 1.85 mm connectors.[32,33] The thus obtained spectra were complemented at frequencies at 10 MHz to 400 MHz using a cut-off type coaxial cell.[34,35] All experiments were performed at ambient temperature (295 ± 2 K).

To obtain information on the chemical environment of Qu we performed a set of NMR experiments. ^{1}H NMR spectra of the solutions were recorded on a Bruker 300, 500 and 850 MHz AVANCE III spectrometer. For selected samples we recorded both ^{1}H- and ^{31}P-NMR spectra using a 5 mm BBFO *z*-gradient probe on the 500 MHz Bruker AVANCE III system (TOPSPIN 3.2 software version). The spectra were obtained with $\pi/2$-pulse lengths of 14.7 μs for proton (128 number of scans, spectra width 12500 Hz) and 12 μs for ^{31}P and a relaxation delay of 3 s for ^{1}H NMR and 10 s for ^{31}P NMR. The proton spectra were referenced using the residual $CDHCl_2$ at 5.37 ppm ($\delta(^1H)$). The ^{31}P spectra were referenced using Triphenylphosphine at −6 ppm.

To extract information on the intermolecular interaction between DPP and Qu we complemented our analysis with two dimensional (2D) ^{31}P–^{1}H HOESY[36] (heteronuclear Overhauser enhancement spectroscopy) methods. The spectroscopic widths of the heteronuclear 2D-HOESY experiments were typically 1600 Hz in the detected dimension (F1 (^{1}H: 10000 Hz) and F2 (^{31}P: 1600 Hz)) using a relaxation delay of 2 s. The mixing time for the HOESY experiment was set to 1500 ms. Information on the hydrodynamic size of the molecular aggregates in solution was studied using diffusion ordered NMR Spectroscopy (DOSY-NMR). These spectra were recorded using a 5 mm TXI ^{1}H/^{13}C/^{15}N *z*-gradient probe with a gradient strength of 5.350 [G mm^{-1}] on a Bruker Avance-III 850 NMR Spectrometer. The gradient strength of the probes was calibrated by analysis of a sample of $^2H_2O/^1H_2O$ and compared to the reported diffusion coefficient of $^2H_2O/^1H_2O$ (values taken from Bruker diffusion manual) at 298.3 K. In this work, the gradient was varied using 32 steps from 2% to 100% and the diffusion time was set to 40 ms.

Acknowledgements

C.M. thanks Frederik Fleissner and Vasileios Balos for their assistance with performing and analyzing the DRS experiments. We are grateful to Mischa Bonn for fruitful discussions. This project has received funding from the European Research Council (ERC) under the European Union's Horizon 2020 research and innovation programme (grant agreement n° 714691) and H.K. acknowledges funding within grant agreement n° 658467.

Conflict of interest

The authors declare no conflict of interest.

Keywords: Brønsted acid catalysis · dielectric relaxation spectroscopy · NMR titration · organocatalysis · proton transfer

[1] G. M. Barrow, *J. Am. Chem. Soc.* **1956**, *78*, 5802–5806.
[2] P. M. Tolstoy, P. Schah-Mohammedi, S. N. Smirnov, N. S. Golubev, G. S. Denisov, H.-H. Limbach, *J. Am. Chem. Soc.* **2004**, *126*, 5621–5634.
[3] S. N. Smirnov, N. S. Golubev, G. S. Denisov, H. Benedict, P. Schah-Mohammedi, H.-H. Limbach, *J. Am. Chem. Soc.* **1996**, *118*, 4094–4101.
[4] P. M. Tolstoy, B. Koeppe, G. S. Denisov, H.-H. Limbach, *Angew. Chem. Int. Ed.* **2009**, *48*, 5745–5747; *Angew. Chem.* **2009**, *121*, 5855–5858.
[5] B. Brycki, M. Szafran, *J. Chem. Soc. Perkin Trans. 2* **1982**, 1333.
[6] B. Koeppe, S. A. Pylaeva, C. Allolio, D. Sebastiani, E. T. J. Nibbering, G. S. Denisov, H.-H. Limbach, P. M. Tolstoy, *Phys. Chem. Chem. Phys.* **2017**, *19*, 1010–1028.
[7] B. Koeppe, J. Guo, P. M. Tolstoy, G. S. Denisov, H.-H. Limbach, *J. Am. Chem. Soc.* **2013**, *135*, 7553–7566.
[8] A. Jarczewski, C. D. Hubbard, *J. Mol. Struct.* **2003**, *649*, 287–307.
[9] J. Greindl, J. Hioe, N. Sorgenfrei, F. Morana, R. M. Gschwind, *J. Am. Chem. Soc.* **2016**, *138*, 15965–15971.
[10] M. Fleischmann, D. Drettwan, E. Sugiono, M. Rueping, R. M. Gschwind, *Angew. Chem. Int. Ed.* **2011**, *50*, 6364–6369; *Angew. Chem.* **2011**, *123*, 6488–6493.
[11] H. Kim, E. Sugiono, Y. Nagata, M. Wagner, M. Bonn, M. Rueping, J. Hunger, *ACS Catal.* **2015**, *5*, 6630–6633.
[12] K. Mori, Y. Ichikawa, M. Kobayashi, Y. Shibata, M. Yamanaka, T. Akiyama, *Chem. Sci.* **2013**, *4*, 4235–4239.
[13] N. Sorgenfrei, J. Hioe, J. Greindl, K. Rothermel, F. Morana, N. Lokesh, R. M. Gschwind, *J. Am. Chem. Soc.* **2016**, *138*, 16345–16354.
[14] S. Sharif, E. Fogle, M. D. Toney, G. S. Denisov, I. G. Shenderovich, G. Buntkowsky, P. M. Tolstoy, M. C. Huot, H.-H. Limbach, *J. Am. Chem. Soc.* **2007**, *129*, 9558–9559.
[15] A. Staib, D. Borgis, J. T. Hynes, *J. Chem. Phys.* **1995**, *102*, 2487–2505.
[16] D. W. C. MacMillan, *Nature* **2008**, *455*, 304–308.
[17] K. Brak, E. N. Jacobsen, *Angew. Chem. Int. Ed.* **2013**, *52*, 534–561; *Angew. Chem.* **2013**, *125*, 558–588.
[18] D. Parmar, E. Sugiono, S. Raja, M. Rueping, *Chem. Rev.* **2014**, *114*, 9047–9153.
[19] T. Akiyama, J. Itoh, K. Yokota, K. Fuchibe, *Angew. Chem. Int. Ed.* **2004**, *43*, 1566–1568; *Angew. Chem.* **2004**, *116*, 1592–1594.
[20] I. D. Gridnev, M. Kouchi, K. Sorimachi, M. Terada, *Tetrahedron Lett.* **2007**, *48*, 497–500.

[21] M. N. Grayson, J. M. Goodman, *J. Am. Chem. Soc.* **2013**, *135*, 6142 – 6148.
[22] T. Marcelli, P. Hammar, F. Himo, *Chem. Eur. J.* **2008**, *14*, 8562 – 8571.
[23] J. P. Reid, L. Simón, J. M. Goodman, *Acc. Chem. Res.* **2016**, *49*, 1029 – 1041.
[24] L. Simón, J. M. Goodman, *J. Am. Chem. Soc.* **2008**, *130*, 8741 – 8747.
[25] A. Milo, A. J. Neel, F. D. Toste, M. S. Sigman, *Science* **2015**, *347*, 737 – 743.
[26] M. Rueping, C. Azap, E. Sugiono, T. Theissmann, *Synlett* **2005**, 2367 – 2369.
[27] F. Kremer, A. Schönhals, *Broadband Dielectric Spectroscopy*, Springer, Berlin, **2003**.
[28] R. Buchner, *Pure Appl. Chem.* **2008**, *80*, 1239 – 1252.
[29] M.-M. Huang, K. Schneiders, P. S. Schulz, P. Wasserscheid, H. Weingärtner, *Phys. Chem. Chem. Phys.* **2011**, *13*, 4126 – 4131.
[30] V. Balos, H. Kim, M. Bonn, J. Hunger, *Angew. Chem. Int. Ed.* **2016**, *55*, 8125 – 8128; *Angew. Chem.* **2016**, *128*, 8257 – 8261.
[31] U. Kaatze, *Meas. Sci. Technol.* **2013**, *24*, 012005.
[32] D. V. Blackham, R. D. Pollard, *IEEE Trans. Instrum. Meas.* **1997**, *46*, 1093 – 1099.
[33] W. Ensing, J. Hunger, N. Ottosson, H. J. Bakker, *J. Phys. Chem. C* **2013**, *117*, 12930 – 12935.
[34] O. Göttmann, U. Kaatze, P. Petong, *Meas. Sci. Technol.* **1996**, *7*, 525 – 534.
[35] J. Hunger, N. Ottosson, K. Mazur, M. Bonn, H. J. Bakker, *Phys. Chem. Chem. Phys.* **2015**, *17*, 298 – 306.
[36] C. Yu, G. C. Levy, *J. Am. Chem. Soc.* **1984**, *106*, 6533 – 6537.
[37] M. Rueping, A. P. Antonchick, T. Theissmann, *Angew. Chem. Int. Ed.* **2006**, *45*, 3683 – 3686; *Angew. Chem.* **2006**, *118*, 3765 – 3768.
[38] R. Buchner, G. Hefter, *Phys. Chem. Chem. Phys.* **2009**, *11*, 8984 – 8999.
[39] J. Hunger, A. Stoppa, A. Thoman, M. Walther, R. Buchner, *Chem. Phys. Lett.* **2009**, *471*, 85 – 91.
[40] C. F. J. Böttcher, *Theory of Electric Polarization*, Elsevier, Amsterdam, **1978**.
[41] Note that the formation of H-bonded Qu-DPP aggregates (without proton transfer) can be excluded based on our earlier experiments and ab initio calculations.[11]
[42] We note that in our previous study of equimolar mixtures of DPP and Qu,[11] we used a symmetrically broadened Cole–Cole function (broadened with respect to the Debye function), which subsumed the multimer and the ion pair relaxation in Equation (1). In the present study, the variation of the DPP concentration allows for a separation of both contributions.
[43] N. S. Golubev, G. S. Denisov, S. N. Smirnov, D. N. Shchepkin, H.-H. Limbach, *Z. Phys. Chem. (Muenchen Ger.)* **1996**, *196*, 73 – 84.
[44] F. Giacalone, M. Gruttadauria, P. Agrigento, R. Noto, *Chem. Soc. Rev.* **2012**, *41*, 2406 – 2447.
[45] M. Terada, K. Machioka, K. Sorimachi, *Angew. Chem. Int. Ed.* **2006**, *45*, 2254 – 2257; *Angew. Chem.* **2006**, *118*, 2312 – 2315.
[46] N. Li, X.-H. Chen, S.-M. Zhou, S.-W. Luo, J. Song, L. Ren, L.-Z. Gong, *Angew. Chem. Int. Ed.* **2010**, *49*, 6378 – 6381; *Angew. Chem.* **2010**, *122*, 6522 – 6525.
[47] M. Hatano, K. Moriyama, T. Maki, K. Ishihara, *Angew. Chem. Int. Ed.* **2010**, *49*, 3823 – 3826; *Angew. Chem.* **2010**, *122*, 3911 – 3914.
[48] I. Čorić, B. List, *Nature* **2012**, *483*, 315 – 319.
[49] S. Das, L. Liu, Y. Zheng, M. W. Alachraf, W. Thiel, C. K. De, B. List, *J. Am. Chem. Soc.* **2016**, *138*, 9429 – 9432.
[50] L. Liu, M. Leutzsch, Y. Zheng, M. W. Alachraf, W. Thiel, B. List, *J. Am. Chem. Soc.* **2015**, *137*, 13268 – 13271.

Manuscript received: April 7, 2017
Accepted manuscript online: June 8, 2017
Version of record online: July 24, 2017

